NUMERICAL INVESTIGATION OF NATURAL CONVECTION RADIATION AND MAGNETOHYDRODYNAMIC IN VERTICAL POROUS CYLINDRICAL CHANNEL

Manal H. AL-Hafidh
Ass. Prof. /University of Baghdad

Hayder I. Mohammed
Mechanical Engineer

ABSTRACT

A numerical study has been carried out to investigate heat transfer by natural convection and radiation under the effect of magnetohydrodynamic (MHD) for steady state axisymmetric two-dimensional laminar flow in a vertical cylindrical channel filled with saturated porous media. Heat is generated uniformly along the center of the channel with its vertical surface remain with cooled constant wall temperature and insulated horizontal top and bottom surfaces. The governing equations which used are continuity, momentum and energy equations which are transformed to dimensionless equations. The finite difference approach is used to obtain all the computational results using the MATLAB-7 programming. The parameters affected on the system are Rayleigh number ranging within ($10^2 \leq Ra \leq 10^4$), radiation parameter ($0 \leq Rd \leq 2$) and MHD (Mn) ($0 \leq Mn \leq 2$).
The results obtained are presented graphically in the form of streamline and isotherm contour plots and the results show that heat transfer enhanced by radiation effect but decrease with the increase of magnetohydrodynamic. A correlation has been set up to give the average Nusselt number variation with Ra, Rd and Mn for which the results are found to be in good agreement with previously published researches which give maximum deviation of 3.73% when compared with the results of **(Prasad, 1989).**

دراسة عددية للحمل الحر والإشعاع والمغناطيسية الهيدروديناميكية في قناة عمودية مملؤة بوسط مسامي

الخلاصة

أجريت دراسة رقمية لإستقصاء إنتقال الطاقة الحرارية بالحمل الحر والإشعاع تحت تأثير المغناطيسية الهيدروديناميكية(MHD) لجريان طباقي مستقر ثنائي البعد في مجرى اسطواني عمودي مملوء بوسط مسامي مشبع. طاقة حرارية متولدة بإنتظام في مركز المجرى مع ثبوت درجة الحرارة الباردة على السطح العمودي للمجرى وعزل السطحان الأفقيان العلوي والسفلي. المعادلات التي أستخدمت هي الإستمرارية، الزخم ومعادلة الطاقة وتم تحويلها إلى معادلات لابعدية. أستخدمت طريقة الفروق المحددة للحصول على النتائج بإستخدام برمجية MATLAB-7. المتغيرات المؤثرة على النظام هي رقم رايلي بمدى ($10^2 \leq Ra \leq 10^4$)، تأثير الإشعاع ($0 \leq Rd \leq 2$) والمغناطيسية الهيدروديناميكية (MHD (Mn 0 $\leq Mn \leq 2$).
النتائج تم توضيحها برسم منحنيات مغلقة للخطوط الإنسيابية ومنحنيات درجات الحرارة الثابتة وبينت النتائج أن الإشعاع يعزز من إنتقال الطاقة الحرارية بينما تقل الطاقة الحرارية بزيادة المغناطيسية الهيدروديناميكية. والنتائج أعطت تمثيلاً لمعدل رقم نسلت ضد Ra, Rd وMn . المقارنة مع البحوث الأخرى أعطت نتائج دقيقة كفاية لإمكانية حساب معامل انتقال الطاقة الحرارية لحالة الجريان المذكورة آنفاً وكان الفرق بالنتائج 3.73% بالمقارنة مع نتائج **(Prasad, 199)**

KEY WORDS:- Natural convection, radiation, magnetohydrodynamic, vertical cylindrical channel, laminar flow numerical solution

INTRODUCTION

Various heat transfer mechanisms and geometries have been studied by some engineers and scientists purposely to augment heat transfer in heat exchangers and some other heat transfer equipments. A numerical investigation of natural convection was studied for vertical annulus. **(Prasad and Kulacki, 1984)** studied numerically free convection in a vertical annulus filled with saturated porous media whose vertical walls at constant temperatures and insulated horizontal wall. Convective velocities wrer higher in the upper half than the lower in the annulus and the local rate in the heat transfer much higher near the top edge of the cold wall and Nu was increase with the radius ratio. **(Prasad and Kulacki, 1985)** studied numerically and experimentally the free convection heat transfer in short cylindrical annuli filled with saturated porous media which was glass beads(3 and 6 mm). For an annulus whose inner wall heated with constant temperature and outer wall isothermally cooled, the top and the bottom being insulated. Heat transfer results have been obtained numerically and experimentally up to Ra = 10^4. **(Prasad and Chui, 1989)** studied numerically the natural convection inside a cylindrical enclosure filled with a volumetrically heated, saturated porous medium. Three cases were studied (i) both top and bottom adiabatic, (ii) insulated bottom and cooled top, and (iii) both top and bottom were cooled, and the vertical wall was cooled for all cases. The maximum temperature decreased significantly with the change in horizontal walls boundary conditions from adiabatic to isothermally cool. The lower is the aspect ratio and\or Rayleigh number, the larger the variation in maximum temperature. **(Shivakumara and Prasanna, 2002)** studied numerically the free convection in vertical cylinder annulus filled with fluid saturated porous medium with the inner wall heated to a uniform temperature, the outer wall cooled to a uniform temperature and maintaining top and bottom boundaries at adiabatic condition. The heat transfer rate and the flow field were obtained for $10^3<Ra<10^6$, Darcy number $10^{-1}<Da<10^{-3}$ and aspect ratio 1 to 2. The results show that the heat transfer rate decreased as the Darcy number decreased.
(Rashad, 2007) was studied the magneto-hydrodynamics and radiation effect in study laminar boundary layer flow of Newtonian. Viscous fluid over a vertical flat plate embedded in a fluid saturated porous media in the presence of thermophoresis particle deposition effect. The conclusion deduced that the velocity of the fluid decreased with increasing of magnetic field and buoyancy ratio.

MATHEMATICAL MODEL

The schematic drawing of the geometry and the Cartesian coordinate system employed in solving the problem is shown in **Fig.1.** The fluid flows naturally in the cylinder. This cylinder is symmetrical about z-axis (**$\partial/\partial r=0$**). Convection heat transfer through a saturated porous media with a fluid (liquid or gas) is based on a series of concepts; such concepts include porosity and permeability of the porous media, and the volume average properties of the fluid flowing through the medium. The governing equations for axisymmetric, steady flow through Darcy porous medium including the radiation and magnetohydrodynamic effect are:

Continuity Equation

$$\frac{1}{r}\frac{\partial}{\partial r}(rV_r)+\frac{\partial V_z}{\partial z}=0 \qquad (1)$$

Momentum Equation

In z direction

$$V_z=-\frac{K}{\mu}\left[\frac{\partial p}{\partial z}+\rho g+\sigma\beta_z^2 V_z\right] \qquad (2)$$

In r direction

$$V_r=-\frac{K}{\mu}\left[\frac{\partial p}{\partial r}+\sigma\beta_z^2 V_r\right] \qquad (3)$$

The density of the fluid assumed constant except when it's happened directly from flotation force **(Bejan, 1999).**

$$\left.\begin{aligned}\rho &= \rho_\circ[1-\beta(T-T_\circ)]\\ \beta &= \frac{1}{\rho}\left(\frac{\partial\rho}{\partial T}\right)\end{aligned}\right\} \quad (4)$$

From (4) & (2)

In z direction

$$V_z = -\frac{K}{\mu}\left[\frac{\partial p}{\partial z} + \rho_\circ g[1-\beta(T-T_\circ)] + \sigma\beta_i^2 V_z\right] \quad (5)$$

Energy Equation

According to the assumptions the energy equation and the radiation flux q_r are **(Prasad, 1989)**:

$$V_r\frac{\partial T}{\partial r}+V_z\frac{\partial T}{\partial z}=\frac{k}{\rho Cp}\left[\begin{aligned}&\frac{1}{r}\frac{\partial}{\partial r}\left(r\frac{\partial T}{\partial r}\right)\\ &+\frac{\partial}{\partial z}\left(\frac{\partial T}{\partial z}\right)\\ &-\frac{1}{r}\frac{\partial}{\partial r}\left(\frac{r\,q_r}{k}\right)\end{aligned}\right]+\frac{q^{\circ}}{\rho C_p} \quad (6)$$

$$q_r = -\frac{4\sigma_i\partial T^4}{3\beta_r\partial r}$$

NORMALIZATION PARAMETERS

The variables in the governing equations and boundary conditions are transformed to dimensionless formula by employing the following transformation parameters **(Prasad, 1989):**

$$\bar{r}=\frac{r}{R}\ ,\ \bar{z}=\frac{z}{H}\ ,\ \bar{T}=\frac{T-T_c}{\frac{q''R^2}{zk}}\ ,$$

$$\bar{V}_z=\frac{V_zR^2}{H\alpha} \quad (7)$$

$$\bar{V}_r=\frac{V_rR}{\alpha}\ ,\quad \bar{V}_z=\frac{1}{\bar{r}}\frac{\partial\psi}{\partial\bar{r}}\ ,\quad \bar{V}_r=-\frac{1}{\bar{r}}\frac{\partial\psi}{\partial\bar{z}} \quad (8)$$

By using the relation above the eq. (3, 5 and 6) became

$$\left[A^2\frac{\partial}{\partial\bar{r}}\left(\frac{1}{\bar{r}}\frac{\partial\Psi}{\partial\bar{r}}\right)+\frac{\partial}{\partial\bar{z}}\left(\frac{1}{\bar{r}}\frac{\partial\Psi}{\partial\bar{z}}\right)\right]=\frac{Ra}{1+Mn}A\left[\frac{\partial\bar{T}}{\partial\bar{r}}\right] \quad (9)$$

$$\left[\begin{aligned}&-\left(\frac{1}{\bar{r}}\frac{\partial\Psi}{\partial\bar{z}}\frac{\partial\bar{T}}{\partial\bar{r}}\right)+\\ &\left(\frac{1}{\bar{r}}\frac{\partial\Psi}{\partial\bar{r}}\frac{\partial\bar{T}}{\partial\bar{z}}\right)\end{aligned}\right]=\left[\begin{aligned}&\left(1+\frac{4}{3}Rd\right)\frac{1}{\bar{r}}\frac{\partial}{\partial\bar{r}}\left(\bar{r}\frac{\partial\bar{T}}{\partial\bar{r}}\right)\\ &+\frac{1}{A^2}\left(\frac{\partial^2\bar{T}}{\partial\bar{z}^2}\right)+2\end{aligned}\right] \quad (10)$$

And the boundary condition be

$$\left.\begin{aligned}&\bar{r}=0,\ \Psi=0,\ \frac{\partial\bar{T}}{\partial\bar{r}}=0\\ &\bar{r}=1,\ \Psi=0,\ \bar{T}=0\\ &\bar{z}=0,\ \Psi=0,\ \frac{\partial\bar{T}}{\partial\bar{z}}=0\\ &\bar{z}=1,\ \Psi=0,\ \frac{\partial\bar{T}}{\partial\bar{z}}=0\end{aligned}\right\} \quad (11)$$

Overall Heat Transfer

For the problem considered here, there is no well-defined characteristic temperature difference to express the heat transfer coefficient. However one can define an overall Nusselt number based on either the maximum temperature in the cylinder or the mean temperature in the centerline. When the heat transfer coefficient is defined in terms of $(\bar{T}_{max}-\bar{T}_c)$, the overall Nusselt number is defined as **(Prasad, 1989)**

$$Nu_{max}=\frac{hR}{k}=\frac{1}{\bar{T}_{max}} \quad (12)$$

Nu_{max} It's Nusselt number meaning inverted maximum temperature, and not mean maximum Nusselt number. In a similar way, the average

Nusselt number based on the mean temperature difference $(\bar{T}_{mean}-\bar{T}_c)$ can be expressed as

$$Nu_{mean}=\frac{1}{\bar{T}_{mean}} \quad (13)$$

NUMERICAL SOLUTION

The new algebra equations system can easy be solved using some of known techniques, like relaxation method, to give approximate values of the dependent variables at a number

of discrete points called (grid points or nodes) in the computational domain. A grid was established by subdividing the computational domain in the R and Z directions with indexes i and j that are integers describing the number of radial grid lines from the center of the cylinder and the number of axial grid lines from the lower to upper surface respectively. The spacing of the grid lines in the R-direction is uniform and given by (Δr) and that of the grid lines in the Z-direction is also uniform and given by (Δz). The number of the grid points will be [m×n] where (m) represents the number of gridlines in the R-direction and equals $[(1/\Delta\bar{r})+1]$ while (n) represents the number of gridlines in the Z-direction and equals $[(1/\Delta\bar{z})+1]$.
The partial differential eq. (9) & (10) were finite-differenced using central difference schemes for all of the derivatives. In particular, let ξ represents Ψ and $\bar{T}$ then

$$\Delta\bar{r}=\Delta\bar{z} \quad , \quad \Delta\bar{r}_j=\Delta\bar{r}_{i+1} \quad , \quad \Delta\bar{z}_j=\Delta\bar{z}_{j+1}$$

$$\frac{\partial\xi}{\partial\bar{r}}=\frac{\xi_{(i+1,j)}-\xi_{(i-1,j)}}{2\Delta\bar{r}} \quad , \quad \frac{\partial\xi}{\partial z}=\frac{\xi_{(i,j+1)}-\xi_{(i,j-1)}}{2\Delta\bar{z}} \qquad (13)$$

$$\frac{\partial^2\xi}{\partial\bar{r}^2}=\frac{\xi_{(i+1,j)}-2\xi_{(i,j)}+\xi_{(i-1,j)}}{\Delta\bar{r}^2}$$

$$\frac{\partial^2\xi}{\partial z^2}=\frac{\xi_{(i,j+1)}-2\xi_{(i,j)}+\xi_{(i,j-1)}}{\Delta\bar{z}^2}$$

In terms of the above expressions momentum and energy equations become

Momentum Equation

$$\frac{A^2}{\bar{r}_{(i)}}\frac{\Psi_{(i+1,j)}-2\Psi_{(i,j)}+\Psi_{(i-1,j)}}{\Delta\bar{r}^2}$$
$$-\frac{A^2}{\bar{r}_{(i)}^2}\frac{\Psi_{(i+1,j)}-\Psi_{(i-1,j)}}{2\Delta\bar{r}}$$
$$+\frac{\Psi_{(i,j+1)}-2\Psi_{(i,j)}+\Psi_{(i,j-1)}}{\bar{r}_{(i)}\Delta\bar{z}^2}=\frac{RaA}{1+Mn}\frac{\bar{T}_{(I+1,J)}-\bar{T}_{(I-1,J)}}{2\Delta\bar{r}} \qquad (14)$$

Energy Equation

$$\frac{1}{\bar{r}_{(i)}}\frac{\Psi_{(i+1,j)}-\Psi_{(i-1,j)}}{2\Delta\bar{r}}*\frac{\bar{T}_{(i,j+1)}-\bar{T}_{(i,j-1)}}{2\Delta\bar{z}}$$
$$-\frac{1}{\bar{r}_{(i)}}\frac{\bar{T}_{(I+1,J)}-\bar{T}_{(I-1,J)}}{2\Delta\bar{r}}*\frac{\Psi_{(i,j+1)}-\Psi_{(i,j-1)}}{2\Delta\bar{z}^2}=\left(1+\frac{4}{3}Rd\right)$$
$$\left[\frac{\bar{T}_{(I+1,J)}-2\bar{T}_{(I,J)}+\bar{T}_{(I-1,J)}}{\Delta\bar{r}^2}+\frac{1}{\bar{r}_{(i)}}\frac{\bar{T}_{(I+1,J)}-\bar{T}_{(I-1,J)}}{2\Delta\bar{r}}\right]+\frac{1}{A^2}\frac{\bar{T}_{(i,j+1,J)}-2\bar{T}_{(i,j)}+\bar{T}_{(I,J-1)}}{\Delta\bar{z}^2}+2 \qquad (15)$$

RELAXATION METHOD

As a solution method for the system of algebraic equations (9) and (10) obtained from the discretization of governing differential equations, iterative relaxation method was used. In relaxation methods, the value of the variable to be used for obtaining the solution in the next iteration is the value in the current iteration plus a fraction of the difference between the current value and the predicted value as follows **(Massarotti et. al., 2003):**

$$\Phi_p^{\zeta+1}=\Phi_p^{\zeta}+\gamma\left(\frac{\sum(a_{\zeta b}*\Phi_{\zeta b})+b}{a_p}-\Phi_p^{\zeta}\right)$$

Where:
$\gamma>0$ is the relaxation factor
$\Phi_p^{\zeta+1}$ is the value of the state variable at node P to be used for the next iteration
Φ_p^{ζ} is the value of the state variable at node P form current iteration
$\Phi_{\zeta b}$ is the values of the variable at the surrounding nodes and ap and b are the constants from the discretized equation.

Relaxation method is a relatively simple method and can be easily altered when changing the grid structure or parameters affecting convergence but, the major disadvantage is the task of choosing the optimum relaxation coefficient (γ) for a given situation. The grid that used in this work was (41*61) for $Ra=10^2$&10^3, and (81*81) for $Ra=10^4$. The grid that used in present work showed in **Fig.(2)**. Generally, the temperature is over relaxed and/or the stream function is under relaxation

RESULTS AND DISCUSSION

The results of numerical modeling have been compared with the notable previously published studies. The results that obtained from these studies gave a good agreement where these results compared with **(Prasad, 1985)** maximum deviation was found (2.81%) and with **(Prasad, 1989)** the maximum deviation was found to be (3.73%). **Table 1 & 2** show the value of the mean Nu of the present work comparing with previous work, with explaining the deviation.

Table 1 Comparison of the present results with that of (Prasad, 1985)

ϵ	Ra	Nu. Prasad	Nu. Present	%Dev.
2.5	90	4.271	4.25	0.491
	30	2.275	2.211	2.81
3.333	105	5.071	5.005	1.3
	35	2.691	2.622	2.56
5	120	6.242	6.188	0.865
	40	3.384	3.41	-0.677

Table 2 Comparison of the present results with that of (Prasad, 1989)

A=1	Nu_{Mean} Prasad	Nu_{Mean} Present	%Dev.
Ra=100	3.155	3.0371	3.73
Ra=1000	7.639	7.5885	0.66
Ra=10000	19.841	19.3853	2.29

Centerline Temperature Distributions

Figs. 3, 4 and 5 show the effect of Rd, Mn and Ra on the centerline temperature distribution, **Fig. 3** shows the temperature variation along the cylinder centerline with increasing of the radiation parameter. Because heat diffusion in the system increase with increasing of Rd and the temperature value in the upper surface is higher than the lower surface the fluid will moved and collected near the upper surface. The temperature in the centerline increase with increasing of the MHD parameter as it is clear in **Fig. 4**, because the force which created from MHD acting in the opposite direction of the force that caused the motion of the fluid and this behavior caused a low diffusion of the heat and increasing of the temperature. In **Fig.5** the dimensionless temperature in the centerline dropped with the increasing of Ra, because of the circulation between the layer of the flow which cause more heat diffusion.

Streamlines and Temperature Fields

The Rd Effect

The Rd effect is presented in **Fig. 6**. When Rd equal zero, that mean's no radiation effect on the system. In **Fig.6** (Ra=100, A=1, Mn=1) the warm region area limited between the centerline and the upper wall of the cylinder and the cold region was adjacent to the cold vertical wall, maximum temperature for internal cell was (0.4263) when the Rd was increased the warm region was contracted from the upper wall and more expanded in the centerline, maximum temperature for internal cell was (0.201) at Rd=1 and (0.124) at Rd=2. The change in the flow was not affected on

the shape too much. This increasing in the hot region area is happen because of the increasing of the flow and heat diffusion in the system, and the value of the stream decrease because the molecular lose it's energy with losing the heat.

The Mn Effect

From **Fig. 7** it is clear that the dimensionless streamlines (Ψ) in the internal cell was dropped from (4.187) at Mn=0 to (2.11) at Mn=2, and the maximum dimensionless temperature line was increased from (0.133) at Mn=0 to (0.184) at Mn=2. From the foregoing it's clear that the streamlines value was dropped with the increasing of Mn at constant value of Ra, A & Rd, because the force which created from MHD acting in the opposite direction of the force that caused the motion of the fluid, and this behavior caused a low diffusion of the heat and increasing of the temperature.

The Ra Effect

From **Fig. 8** for (A=1, Rd=1 & Mn=2) it's clear that the temperature of the hotter region was decreased with the increasing of Ra, where this temperature equal to (0.196) at $Ra=10^2$ and (0.088) at $Ra=10^4$, taking part (b) of the last figures, it's clear that the streamlines value in the internal cell increased with the increasing of Ra, where this streamlines equal to (0.257) at $Ra=10^2$ and (8.151) at $Ra=10^4$. This behavior was happened because the increasing of the Ra cause an increasing in the velocity and more circulation between the layers of the fluid that caused the temperature to be dropped.

Mean (Nu) Number and Maximum Temperature

As can be expected the temperature is always maximum in the center of the upper surface. **Fig.9** illustrates the variation of (T_{max} and Nu_{mean}) with Mn respectively at $Ra=10^4$ and A=1 for different values of Rd, it's clear that the value of the maximum temperature was decreased with the increase of Rd at a certain value of Mn, and that the value of the mean Nusselt number (at a certain value of Ra and Mn) was increase with Rd increasing because the increase of the radiation caused increasing of the heat flux diffusion. **Fig.10** shows the variation of (T_{max} & Nu_{mean}) with Rd respectively at $Ra=10^3$ for different values of Mn, it's clear that the value of the maximum temperature was increased with the increasing of Mn at a certain value of Rd and that the value of the mean Nusselt number at a certain value of Ra and Rd, was decreased with Mn increasing.

A correlation was deduced from the numerical data for cases 1 and 2 which is given as:

$$Nu_{mean} = a\ Ra^{b}\ A^{c}\left(\frac{1}{1+Mn}\right)^{d}\left(\frac{1}{1+Rd}\right)^{e}$$

	a	b	c	d	e
Case 1	1.4	0.222	-0.282	0.2168	-0.6588
Case 2	2.68	0.252	-0.877	0.2391	-0.329

CONCLUSIONS

1. Isothermal lines and the streamlines are symmetric about vertical center line. The maximum temperature was appeared at the centerline of the top surface.
2. Temperature and stream were decrease, Nu_{mean} was increase, and the hot region area and inner streamlines cells was increased with increasing of Rd.
3. With increasing of Mn the temperature was increased and the streamline was dropped. Nu_{mean} was decreased with Mn increase.
4. Temperature was decreased and the streamline and Nu_{mean} was increased with increasing of Ra, for high values of Ra the warm region will be adjacent to the upper wall.
5. At a low Ra there are a little change of T_{max} and Nu_{mean} with Mn at constant Rd and A.

REFRENCES

Bejan A. and Nield D., (1999), "Convection in Porous Media", Springer

Massarotti N., Nithiarasu P. and Carotenuto A., (2003), "Microscopic and Macroscopic Approach for Natural Convection in Enclosures Filled with Fluid Porous Medium", Int. J. of Numerical Methods for Heat and Fluid Flow, Vol.13, No.7, pp. 862-886.

Prasad , V. and Kulacki, F. A., (1984), "Natural convection in a vertical porous annulus", Int. J. Heat Mass Transfer. Vol. 27 No. 2, PP (207-219).

Prasad, V. and Kulacki, F. A., (1985), "Natural convection in porous media bounded by short concentric vertical cylinders", Transaction of ASME, J. of heat transfer , Vol. 107, PP (147-154), February.

Prasad, V. and Chui, A., (1989), "Natural convection in cylindrical porous enclosure with internal heat generation", Transaction of ASME, J. of heat transfer, Vol. 111, PP (916-925), November,.

Rashad A. M., (2007), "Influence of radiation on MHD free convection from a vertical flat plate embedded in porous media with thermophoretic deposition of particles", Communication in nonlinear science and numerical simulation www.sciencedirect.com.

Shivakumara, I. S.,and Prasanna, B. M. R., (2002), "Numerical Study of Natural Convection in a Vertical Cylindrical Annulus Using Non-Darcy Equation", J. of Porous Media, Vol.5, No.2, PP.87-102.

NOMENCLATURE

Symbols	Description	Units
As	Dimensionless aspect ratio (A = H/R)	
C_p	specific heat at constant Pressure	J/kg.K
Da	Darcy number (Da = K/R^2)	
g	Acceleration of gravity	m/s^2
H	axial length of cylinder	m
h	Heat transfer coefficient	$W/m^2.K$
K	Permeability	m^2
k	Thermal conductivity	W/m.K
M_n	Magnetohydrodynamic parameter ($M_n = K\sigma\beta_*^2/\mu$)	m^3s/kg
Nu	Nusselt number (Nu=h.R/k)	
Nu_{mean}	Average Nusselt number	
Nu_{max}	Nusselt number resulting from inverted maximum temperature	
p	Pressure	N/m^2
$\dot{q}$	volumetric heat generation	W/m^3
q_r	Radiation flux	W/m^2
T	Temperature	°C
$\overline{T}$	Dimensionless temperature ($\overline{T} = \frac{2k(T-T_c)}{\dot{q}R^2}$)	
T_*	Reference temperature	°C
Tc	Cooled temperature for boundary	°C
$\overline{T}_{max}$	Dimensionless maximum temperature	
$\overline{T}_{mean}$	Dimensionless mean temperature	
R	Radius of the cylinder	m
Ra	Rayleigh number ($Ra = \frac{K\rho g\beta \dot{q} R^3}{2\mu\alpha k}$)	
Rd	Radiation parameter ($Rd = \frac{4\sigma_1 T_\infty^3}{\beta k}$)	
r	Radial coordinate	m

$\bar{r}$	Dimensionless Radial coordinate	
U	Average velocity of the flow	m/s
Vr	Radial velocity component	m/s
$\bar{V}$	velocity vector	
Symbols	Description	Units
$\bar{v}_r$	Dimensionless radial velocity component $(\bar{V}_r = \frac{V_r R}{\alpha})$	
Vz	Axial velocity component	m/s
$\bar{v}_z$	Dimensionless axial velocity component $(\bar{V}_z = \frac{V_z R^2}{\alpha H})$	
z	Axial coordinate	m
$\bar{z}$	Dimensionless axial coordinate	

GREEK SYMBOLS

Symbols	Description	Units
α	Convective thermal diffusivity	m2/s
β	Volumetric thermal expansion coefficient	1/K
β_0	Strength of magnetic field	
β_r	Roseland extinction coefficient	1/m
ε	Porosity	
$\forall$	Total volume of porous media	m3
$\forall_p$	Solid matter volume	m3
$\forall_0$	Difference between $\forall$ & $\forall_p$	m3
σ	Electrical conductivity of the fluid	
σ_i	Stephan Boltzmann constant	W/m2.K4
□	Dimensionless Stream function	
γ	Relaxation factor	
ξ	Represents ψ and $\bar{T}$	
ψ	Stream function	m2/s
Δ	Difference between two values	
μ	Dynamic viscosity	kg/m.s
∇	Laplacian in dimensionless cylindrical coordinates	
η	Actual value of the quantity of a point inside the sample volume	
ρ_0	Reference density at T_0	kg/m3
Φ_p	Value of the state variable at node	

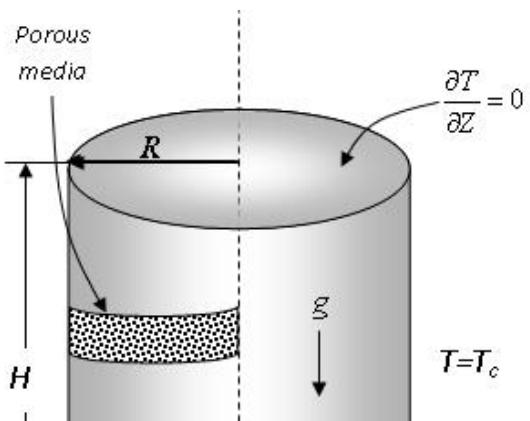

Figure (1) geometric configuration, coordinate system and the boundary conditions

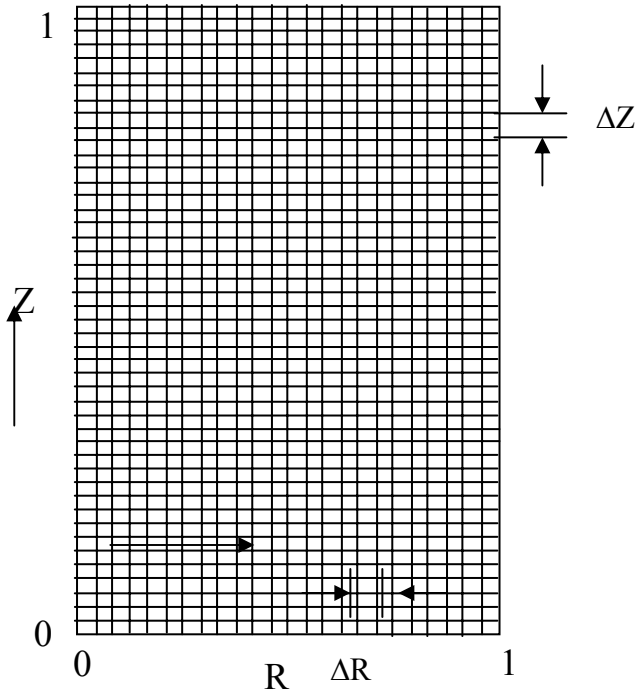

Figure (2) Domain Discretization in a cylindrical enclosure at A=1

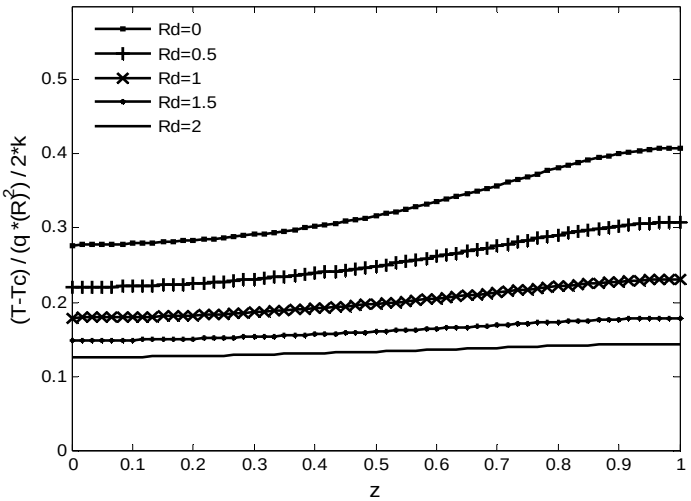

Fig. (3) Effect of Rd on the Temperature distributions at the centerline of the cylinder for (Ra=100, A=1 and Mn=0)

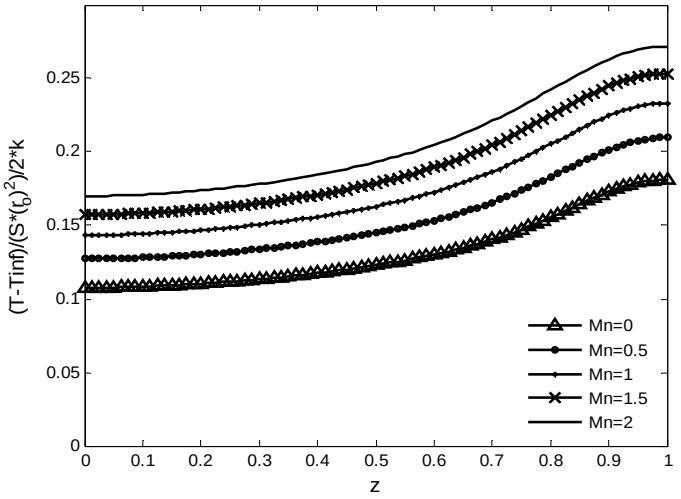

Fig. (4) Effect of Mn on the Temperature distributions at the centerline of the cylinder for (Ra=1000, A=1 and Rd=0)

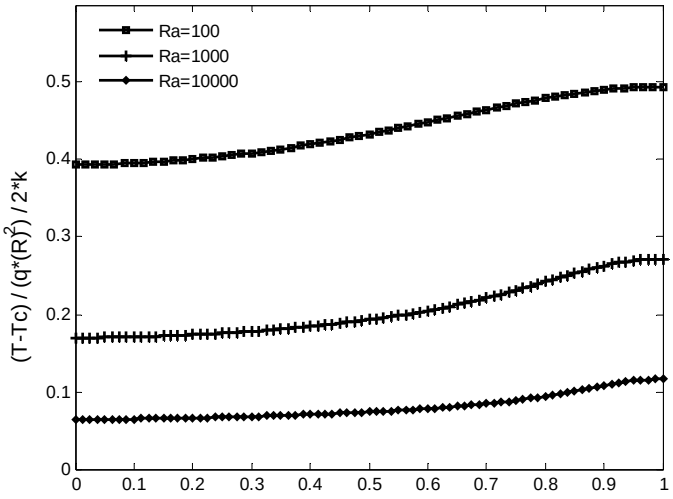

Fig (5) Effect of Ra on the Temperature distributions at the centerline of the cylinder for (Rd=0, A=1 and Mn=2)

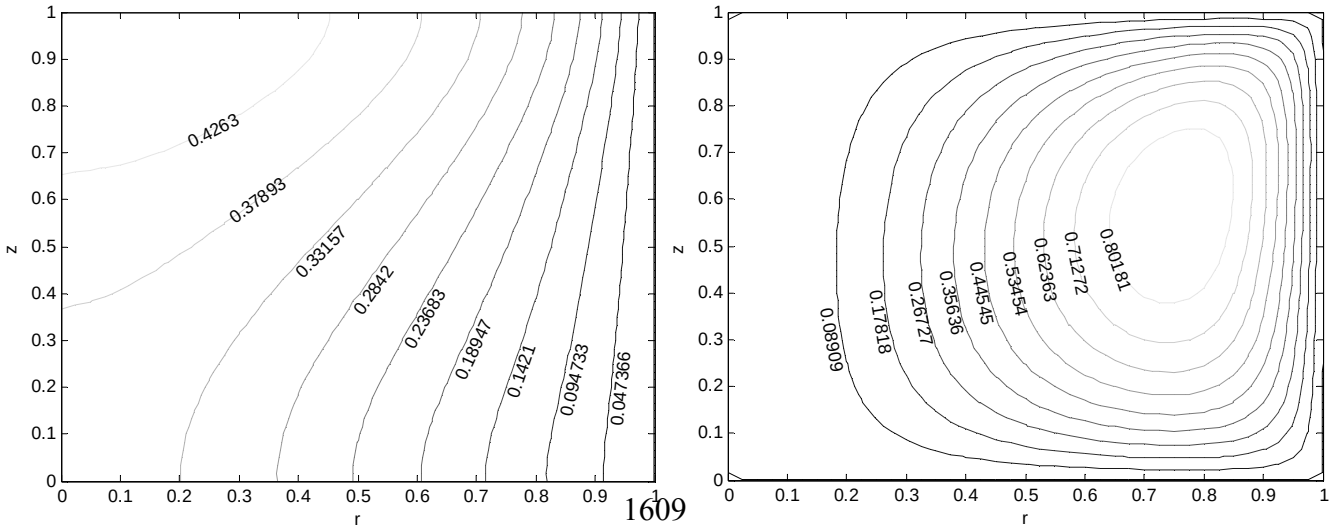

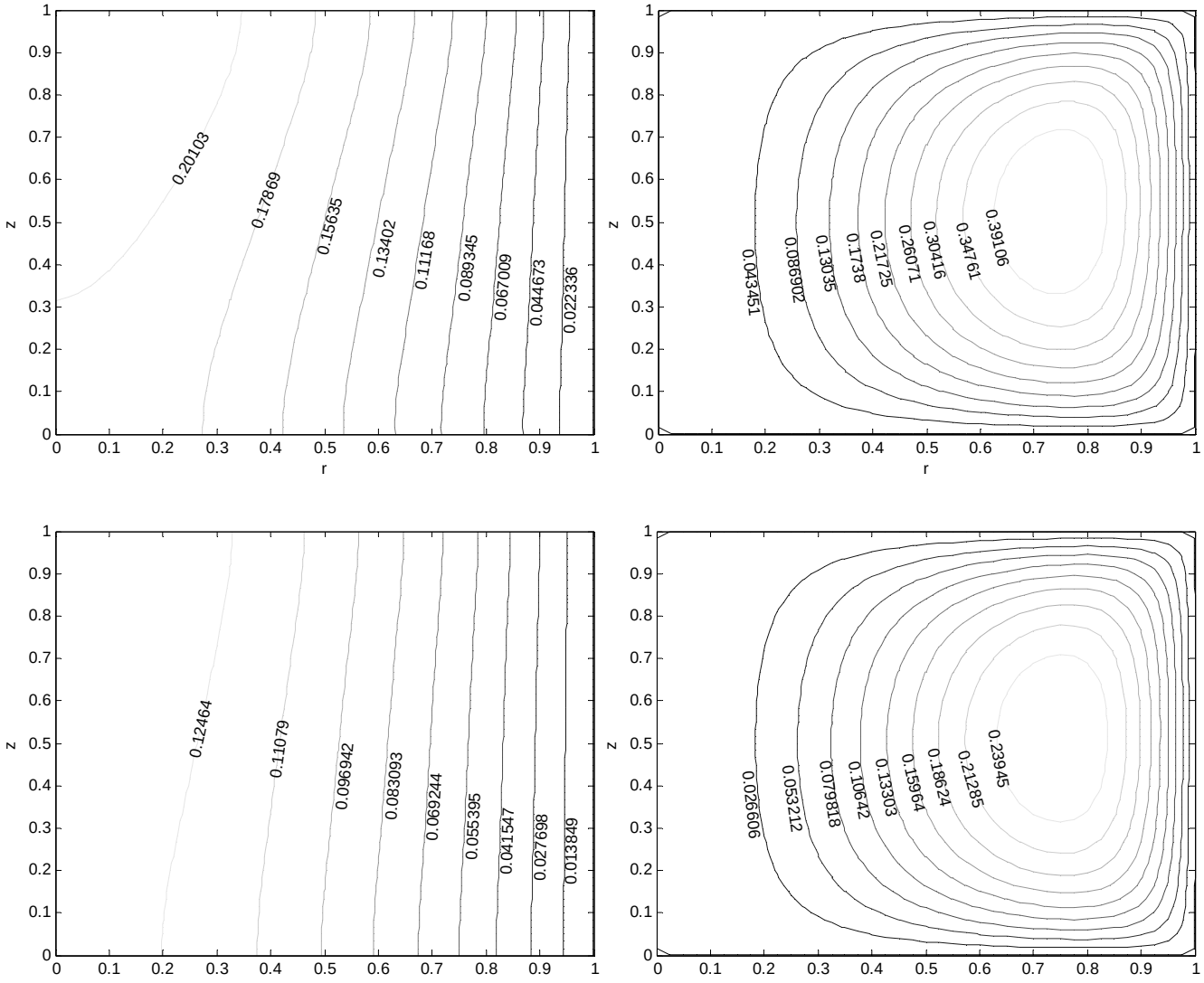

Fig (6) Effect of Rd on the Temperature and fluid flow contours Ra=100, A=1, Mn=1

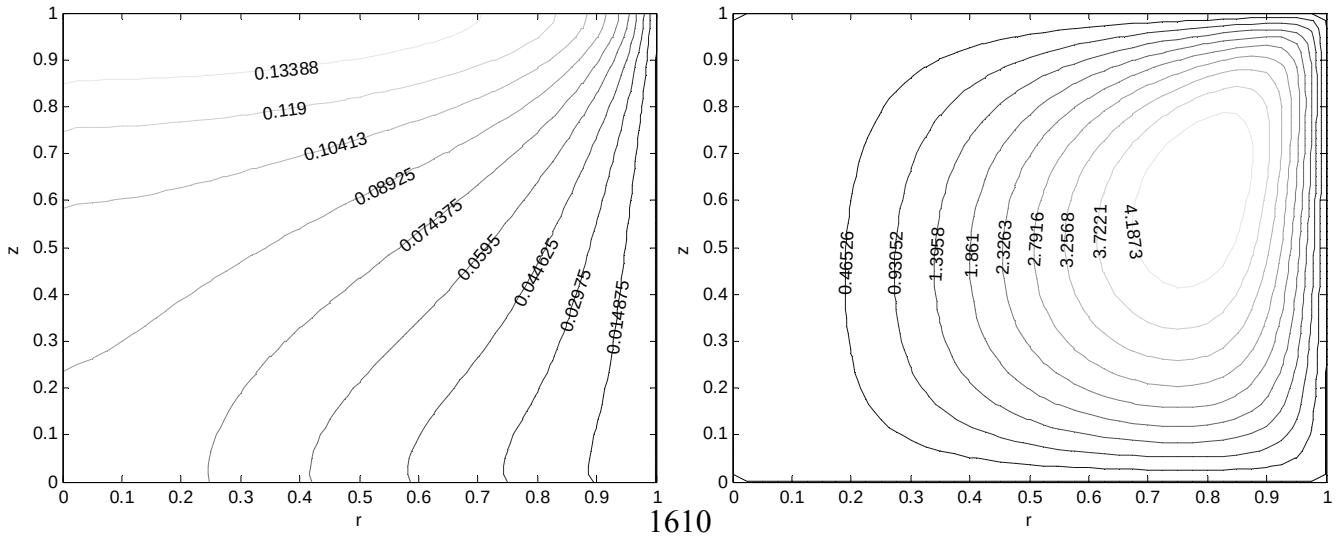

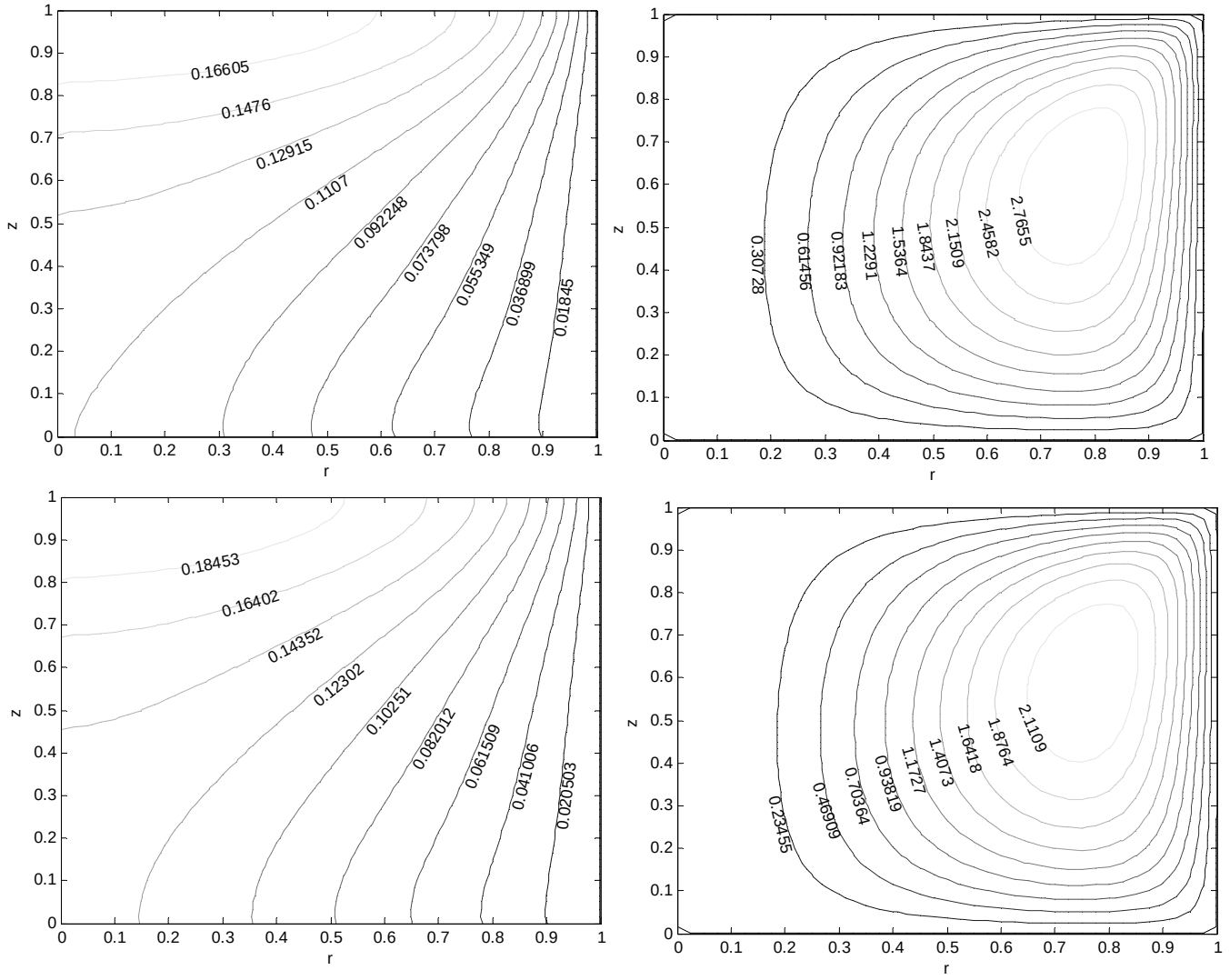

Fig (7) Effect of Mn on the Temperature and fluid flow contours Ra=1000, A=1, Rd=1

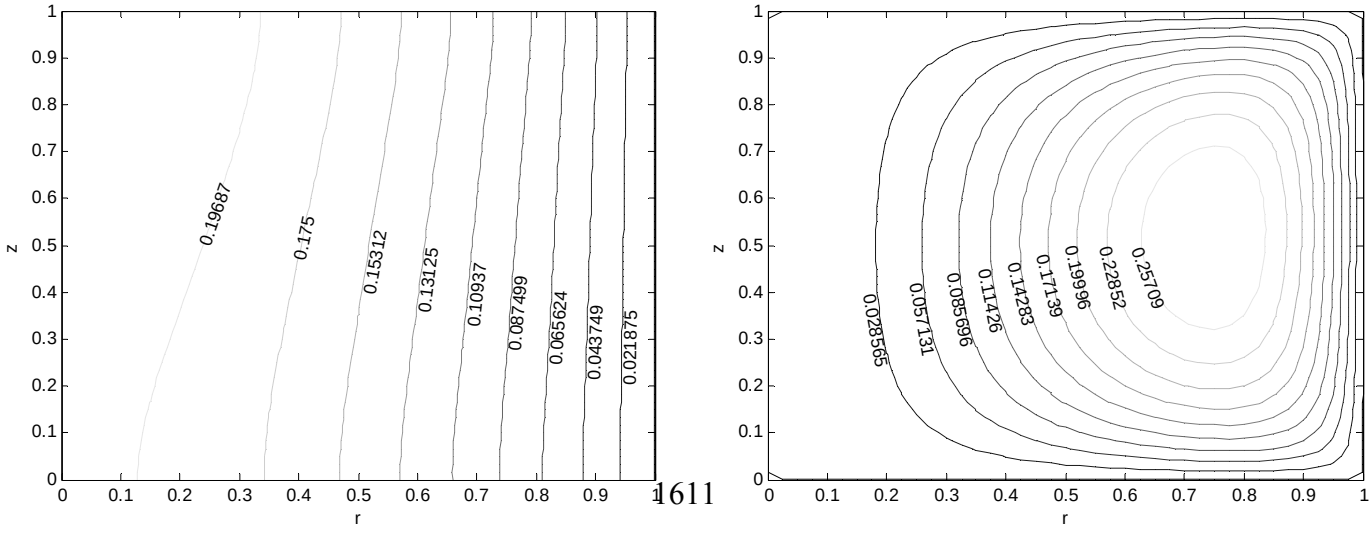

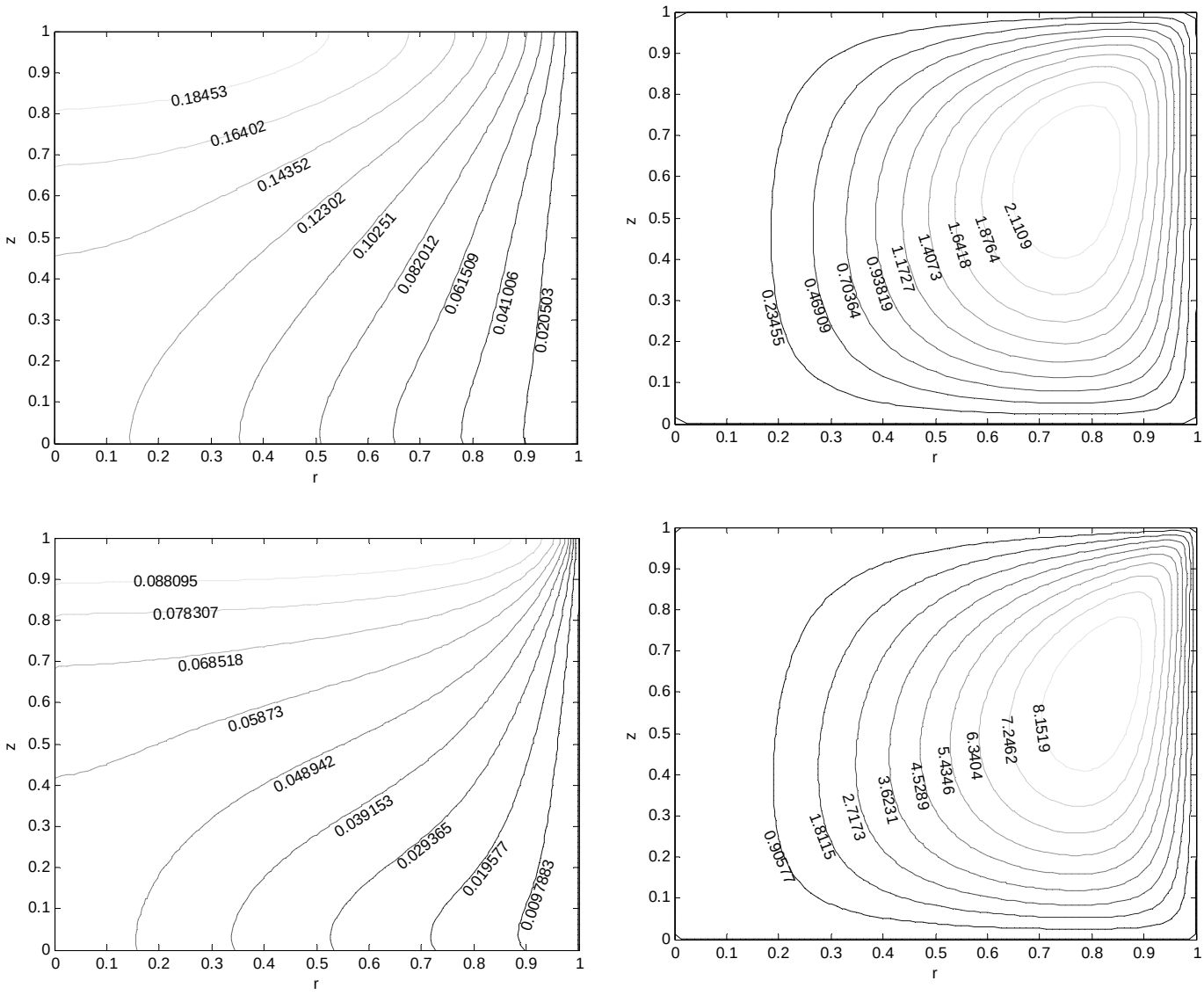

Fig (8) Effect of Ra on the Temperature and fluid flow contours Rd=1, A=1, Mn=2

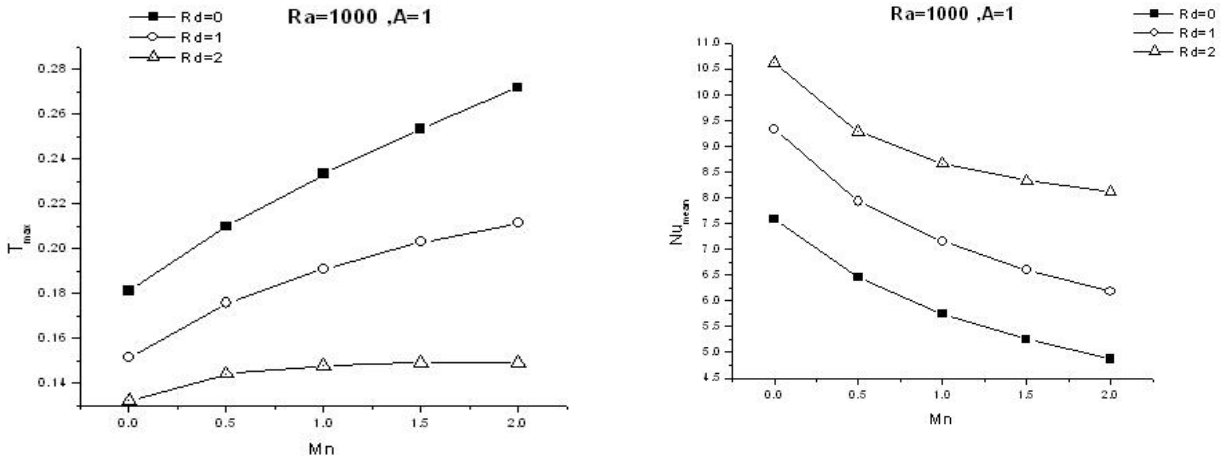

Fig. (9) Effect of Rd on the relationship between T_{max},Nu_{mean} with Mn at Ra=1000 & A=1

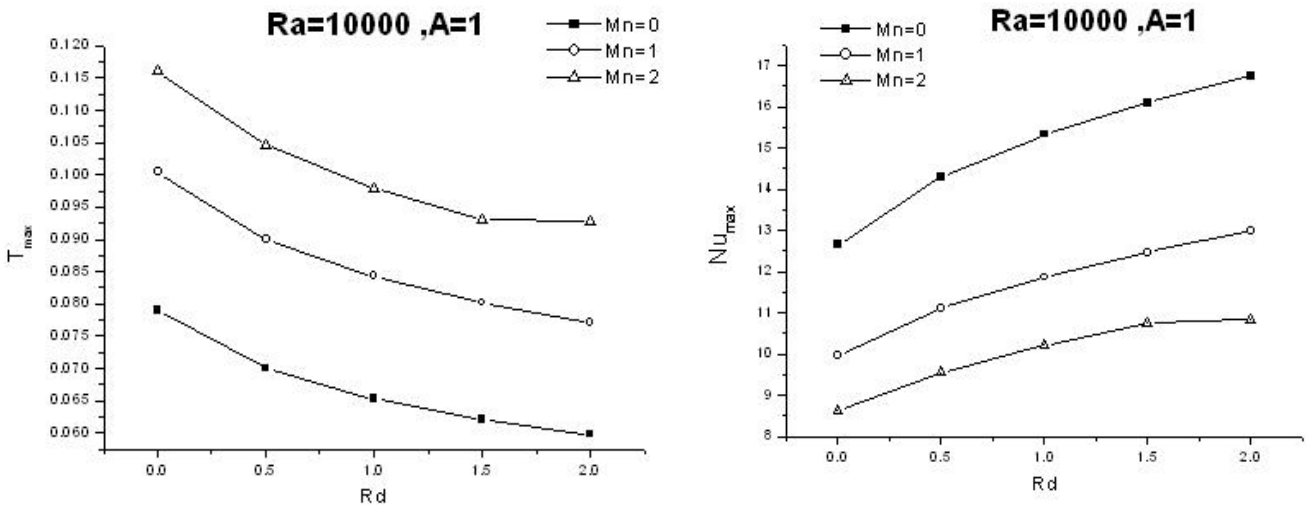

Fig (10) Effect of Mn on the relationship between T_{max},Nu_{mean} with Rd at Ra=10000 & A=1

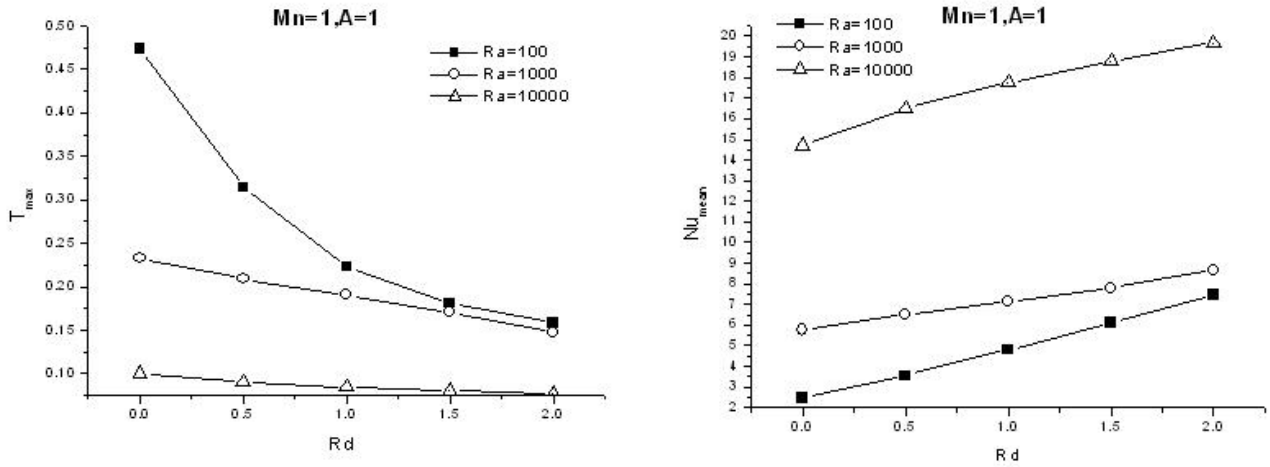

Fig. (11) Effect of Ra on the relationship between T_{max},Nu_{mean} with Rd at A=1 & Mn=1